13th International Symposium on Turbulence and Shear Flow Phenomena (TSFP13)
Montreal, Canada, June 25–28, 2024

THE BALANCE OF POWER IN CONTROLLED CHANNEL FLOW: LIMITS AND POSSIBILITIES

Leo Mangalath
Department of Mechanical Engineering
University of Houston
Houston, TX 77204, USA
lmangalath@uh.edu

Daniel Floryan
Department of Mechanical Engineering
University of Houston
Houston, TX 77204, USA
dfloryan@uh.edu

ABSTRACT

We show that for flow in a channel driven by pressure, shear, or any combination of the two, and controlled via wall transpiration or spanwise wall motion, the uncontrolled laminar state requires the least net energy (accounting for the energetic cost of control). Thus, the optimal control solution is to laminarize the flow. Additionally, we raise the possibility of beating this limit. By simultaneously applying wall transpiration and spanwise wall motion, we show that it may be possible to attain sustained sub-laminar energy expenditure in a controlled flow. We provide a necessary design criterion for net energy savings. In a preliminary set of direct numerical simulations, net energy savings relative to the uncontrolled laminar flow prove elusive, although it is anticipated that larger values of the Reynolds number will provide better opportunities for energy savings.

INTRODUCTION

In flows encountered by airplanes, ships, and pipelines, viscous drag is the main culprit constraining speed and efficiency, and also contributes to wear. Roughly 50–60% of the total drag experienced by cruising aircraft, for example, is attributed to viscous drag (Ricco *et al.*, 2021). Thus, a large fraction of energy expended by these technologies is spent combating viscous drag; even modest reductions in drag could yield significant performance and economic benefits. Accordingly, significant effort has been—and is being—put forth to develop flow control strategies to reduce energy expenditure via viscous drag reduction.

The various flow control approaches have demonstrated varying degrees of success, and new approaches are continually being explored in order to push the boundaries of performance. It is natural to ask which approach is best. This question is best phrased in terms of net energy savings; that is, how much net energy can be saved via control? Phrasing the question as such accounts for the cost of applying control, which is important for active control approaches. A recent review notes that passive approaches have been able to achieve $O(10\%)$ turbulent drag reduction at best, while active approaches have been able to achieve significantly greater drag reduction of up to $\sim 40\%$ (Luchini & Quadrio, 2022). However, the large drag reduction of active approaches is offset by the required energy input. Recent best efforts using spanwise surface oscillations have been able to attain net energy savings of 5–10% in turbulent flows (Marusic *et al.*, 2021; Chandran *et al.*, 2023).

Ultimately, the achievable net energy savings of active flow control approaches must encounter a limit. What has emerged is that when controlling a flow via transpiration (suction and blowing), net energy expenditure is bounded from below by the uncontrolled laminar flow, at least for pressure-driven flow (Bewley, 2009; Fukagata *et al.*, 2009). In other words, the laminar flow is the most energy-efficient and represents a fundamental limitation to the possible energy savings that can be achieved by flow control. It is widely believed that this energy efficiency limit cannot be broken and presents a fundamental impediment to what can be achieved by flow control (Kim, 2011; Jovanović, 2021; Luchini & Quadrio, 2022). We speculate that this energy efficiency limit may be partly responsible for the gradual shift in research effort over the years from control based on transpiration to control based on spanwise wall oscillations.

Here, our contributions are threefold. First, we show that the energy efficiency limit for transpiration-controlled flow extends to flows driven by shear or by an arbitrary combination of pressure and shear. Second, we show that the same energy efficiency limit holds for flows controlled by arbitrary spanwise wall oscillations. Last, we show that by combining transpiration and spanwise wall oscillations, it may be possible to beat the energy limit and sustain sub-laminar energy expenditure. We detail an initial set of direct numerical simulations where we attempt to achieve sub-laminar net energy expenditure.

THEORY

Consider a constant-density flow in a straight channel bounded at the top and bottom by walls. The bottom wall moves with a constant velocity $U_{\text{bot}}\mathbf{i}$, the top wall moves with a constant velocity $U_{\text{top}}\mathbf{i}$, and we impose a pressure gradient

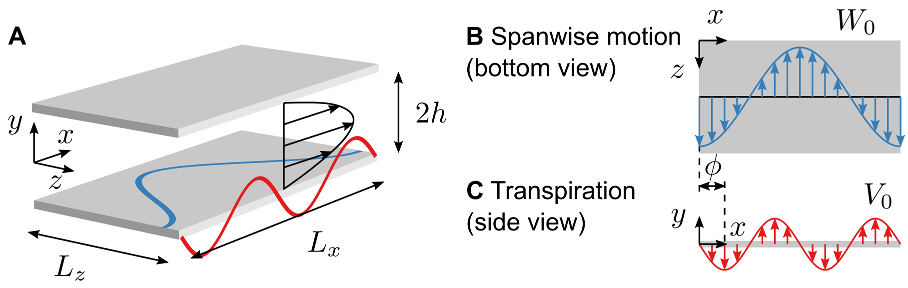

Figure 1. (a) Schematic of flow through a controlled channel. The flow is driven by pressure, and control is applied at the bottom surface. (b) The bottom wall moves in the spanwise direction, with the motion taking the form of a travelling wave. (c) Transpiration is applied at the bottom wall in the form of a travelling wave.

$P_x\mathbf{i}$, where $\mathbf{i}$ is the unit vector in the streamwise direction. The pressure gradient is uniform in space but may depend on time, adjusted such that the bulk velocity U_B is constant. We use periodic boundary conditions in the streamwise and spanwise directions, and no-slip boundary conditions on the walls.

At the walls, we apply control in two forms: transpiration and spanwise wall motion (i.e., Dirichlet boundary conditions on the y and z components of velocity). We allow the controls to have arbitrary spatial and temporal distributions, and require that the net mass flux through the walls is zero.

The uncontrolled laminar flow has a velocity field

$$\mathbf{u}_L = u_L\mathbf{i} = \left[\frac{P_x(y^2-h^2)}{2\mu} + \frac{(U_{\text{top}}-U_{\text{bot}})y}{2h} + \frac{U_{\text{top}}-U_{\text{bot}}}{2}\right]\mathbf{i},$$

where h is the half-height of the channel and μ is the viscosity of the fluid. Work is done to maintain the bulk velocity and to move the walls against forces.

Following Floryan (2023), a control volume analysis leads to the following balance of power in the flow:

$$P_c - P_L = \mu\langle\|\nabla\mathbf{u}'\|^2\rangle - \rho\left\langle\int_{\text{walls}} w^2(\mathbf{u}\cdot\mathbf{n})\,\mathrm{d}A\right\rangle.$$

Above, ρ is the fluid's density, $\mathbf{u}$ is the velocity vector, $\mathbf{u}'$ is the difference between $\mathbf{u}$ and the velocity in the laminar flow without control ($\mathbf{u}' = \mathbf{u} - \mathbf{u}_L$), $\mathbf{n}$ is an outward unit normal vector, and w is the spanwise component of the velocity.

The first term on the left-hand side is the mean power required to maintain the controlled flow; it accounts for the energy needed to apply any mean pressure gradient that is present, the energy needed to power the transpiration (which includes work done against pressure and the injection of kinetic energy into the flow), and the energy needed to power the spanwise surface motion. The second term on the left-hand side is the power needed to maintain the uncontrolled laminar flow, i.e., the steady Stokes flow when there is no transpiration or spanwise surface motion. Together, the two terms on the left-hand side are the difference in power needed to maintain the controlled and uncontrolled flows. Positive values of the left-hand side indicate that the controlled flow is energetically more expensive to maintain than the uncontrolled flow. Conversely, negative values indicate that the control induces net energy savings relative to the uncontrolled laminar flow.

On the right-hand side, angled brackets denote time-averaged quantities. The first term gives the increase in dissipation in the entire domain that is induced by the control. The second term can be interpreted as the covariance between the square of the spanwise speed and the transpiration speed; that is, as the covariance between the two forms of control. Physically, this term originates from the work done on the walls to maintain their motions. Specifically, it is the work associated with the component of the external force that arises due to the momentum flux across the walls.

Note that the above analysis also holds for open channel flows where the top boundary has free-slip and impermeable boundary conditions instead of being a no-slip wall. These boundary conditions were used in the large-eddy simulations of Marusic *et al.* (2021) and Rouhi *et al.* (2023) when investigating streamwise-travelling waves of spanwise surface motion. Since such boundary conditions are uncommon in studies investigating the use of transpiration and spanwise surface motion for control, we say no more about them.

We deduce the following criterion for sustained net energy savings relative to the uncontrolled laminar flow:

$$\rho\left\langle\int_{\text{walls}} w^2(\mathbf{u}\cdot\mathbf{n})\,\mathrm{d}A\right\rangle > \mu\langle\|\nabla\mathbf{u}'\|^2\rangle. \tag{1}$$

One can immediately see that the left-hand side is zero when only transpiration ($w \equiv 0$) or only spanwise surface motion ($\mathbf{u}\cdot\mathbf{n} \equiv 0$) are used for control. Since the right-hand side is non-zero, net energy savings relative to the uncontrolled laminar flow are not possible. This is a generalized form of the fundamental limits given in Bewley (2009) and Fukagata *et al.* (2009).

When transpiration and spanwise surface motion are applied simultaneously, however, the left-hand side of Eq. (1) is capable of being positive, leading to the possibility of sustained net energy savings relative to the uncontrolled laminar flow. The criterion in Eq. (1) is constructive since the left-hand side only depends on control terms. As a result, we can design a pattern of control that guarantees that the left-hand side is positive. This provides a necessary condition for net energy savings. Although we can construct a control scheme that meets the necessary condition, we cannot determine *a priori* whether the control scheme will induce additional dissipation greater than the covariance term. To determine the overall balance of power, we must either perform experiments or simulations.

COMPUTATIONAL RESULTS

We perform direct numerical simulations of pressure-driven flow with control applied at the bottom wall (Figure 1). We use no-slip boundary conditions at the walls and periodic boundary conditions elsewhere.

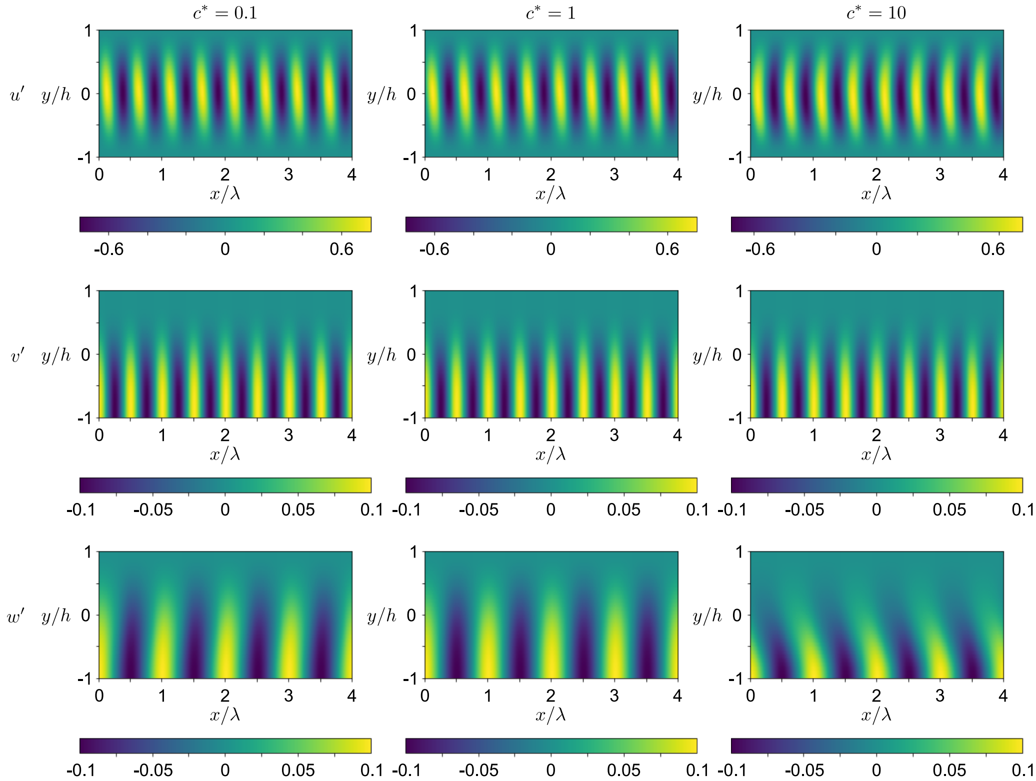

Figure 2. Perturbation velocity in the frame of reference moving with the travelling waves, for $k^* = 0.1$ Each row shows a different velocity component, and each column corresponds to a different wave speed.

The control takes the form of streamwise-travelling waves for the wall-normal and spanwise velocity components,

$$v(x,y,z,t)|_{\text{wall}} = V_0 \cos(k_1 x - \omega_1 t - \phi),$$
$$w(x,y,z,t)|_{\text{wall}} = W_0 \cos(k_2 x - \omega_2 t),$$

which have been independently studied in prior work and have shown better energy efficiency than stationary and uniform distributions of control (Luchini & Quadrio, 2022). This offers direct control of boundary conditions. The net energy expenditure, accounting for the energy required by the control, is measured and compared to that of the uncontrolled case ($V_0 = W_0 = 0$) with an equal streamwise mass flow rate.

For streamwise-travelling waves of transpiration and spanwise surface motion, it can then be shown that sustained sub-laminar net energy expenditure is only possible when

$$V_0, W_0 \neq 0, \quad k_1 = 2k_2, \quad \omega_1 = 2\omega_2,$$

so we limit ourselves to such cases. Physically, the pattern of spanwise surface motion must have twice the wavelength of the pattern of transpiration, and the two must have the same wave speed, as sketched in Figure 1. This establishes that a degree of coherence between the two modes of control is necessary for net energy savings relative to the uncontrolled laminar flow. Limiting ourselves to these coherent patterns leaves us with five control parameters: $k = k_2$, $c = \omega_2/k_2$, ϕ, V_0, and W_0. Additionally, the flow also depends on the Reynolds number.

To perform the simulations, we use the pseudo-spectral solver Dedalus (Burns *et al.*, 2020). Our initial simulations are for a Reynolds number of 10, wave speed $c^* \in \{0.1, 1, 10\}$, wavenumbers $k^* \in \{0.1, 1, 10\}$, phase offset $\phi = 0$, transpiration amplitude $V_0^* = 0.1$, and spanwise amplitude $W_0^* = 0.1$. The bulk velocity has been used as the velocity scale, and the half-height of the channel as the length scale. We numerically solve the Navier-Stokes equations in a frame of reference moving with the travelling waves so that the boundary conditions are steady. Our initial simulations are steady and two-dimensional (although all three velocity components are non-zero), reducing the problem to a boundary-value problem. For a two-dimensional–three-component flow, the x- and y-components of the velocity influence the z-component, but the z-component does not influence the others; that is, there is one-way coupling between these velocity components.

The perturbation velocity fields (the difference between the velocity field and the laminar velocity field) are shown in Figure 2 for $k^* = 0.1$, in Figure 3 for $k^* = 1$, and in Figure 4 for $k^* = 10$. The velocity fields are shown in the frame of reference moving with the travelling waves.

Several observations can be made. The first is that the streamwise perturbation velocity has the same periodicity as the wall-normal perturbation velocity, not as the spanwise flow. This is not surprising since, as we already stated, the streamwise and wall-normal components are coupled for a two-dimensional-three-component flow, while the spanwise velocity has no effect on them.

Next, we make observations about the extent of the perturbation velocity into the channel in the wall-normal direction. The smaller the wavenumber k^* is, the further the control penetrates into the flow. For the smallest wavenumber $k^* = 0.1$, the streamwise perturbation velocity reaches a magnitude on the order of the bulk velocity in the middle of the channel. The wall-normal and spanwise perturbation velocities also pene-

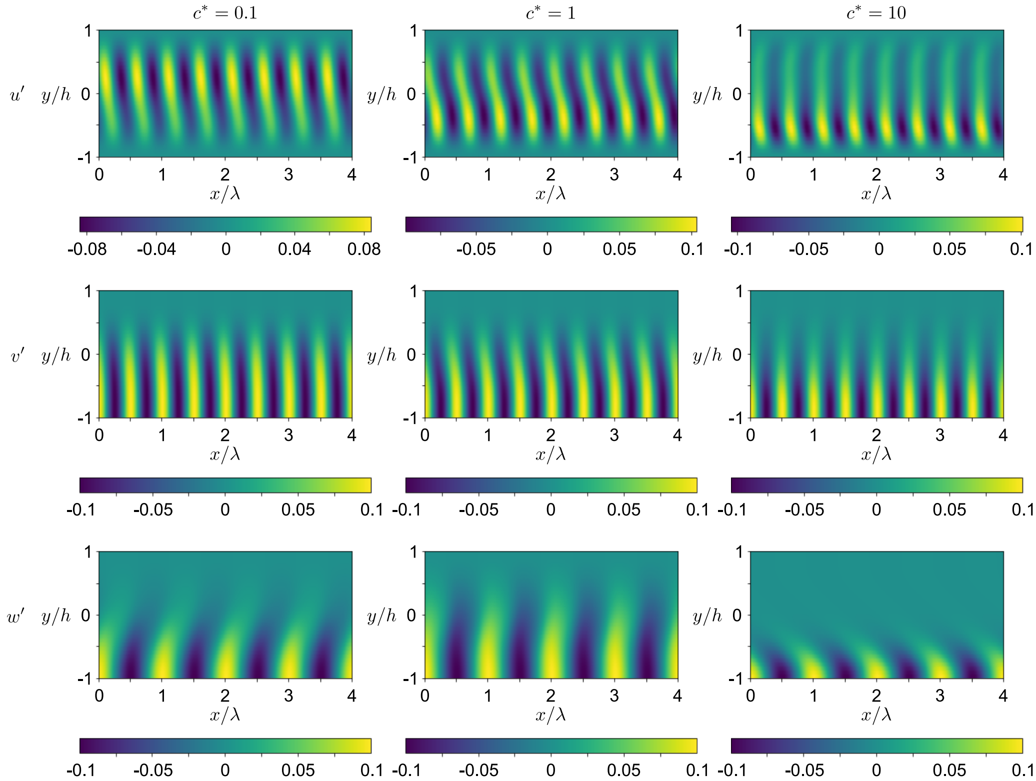

Figure 3. Perturbation velocity in the frame of reference moving with the travelling waves, for $k^* = 1$ Each row shows a different velocity component, and each column corresponds to a different wave speed.

trate deeper into the flow for lower wavenumbers. In contrast, for $k^* = 1$, although the streamwise perturbation velocity spans across the channel, its magnitude is roughly an order of magnitude smaller. For $k^* = 10$, the perturbation velocity field becomes even weaker and localized near the wall where the control is applied.

We can understand the extent of the perturbation velocity into the flow by considering the streamwise and wall-normal velocity components independently of the spanwise velocity, since the spanwise velocity does not affect the other components in this two-dimensional–three-component flow. The oscillatory patterns of the streamwise and wall-normal velocity components have a spatial offset between them in all cases, causing the perturbation flow to consist of counter-rotating circulatory flow regions that intersect the lower wall. Fluid that is injected into the flow through a blowing region on the wall must subsequently be removed through an adjacent suction region. For larger wavenumbers k^*, the distance between adjacent regions of blowing and suction is shorter, so that the injected fluid must turn back into the wall more quickly. The injected fluid therefore spends less time in the channel and cannot penetrate as deeply into the flow. Depending on the strength of the perturbation flow, the total flow may consist of co-rotating regions of circulating flow on the bottom wall, which may act as bearings for the overlying stream. If such a structure can be created, it would have the potential to reduce the overall drag in the flow.

Next, we observe the effect that the wave speed has on the perturbation velocity. The wave speed has a small effect on the penetration depth of the perturbed flow, at least compared to the effect of the wavenumber. This can be seen for $k^* = 1$ and 10, where increasing the wave speed leads to a decrease in the penetration depth. For the largest wavenumber, the largest wave speed also produces a stronger streamwise perturbation velocity compared to the other wave speeds. For $k^* = 0.1$, the perturbation velocity has penetrated across the entire channel, and changing the wave speed has little effect on penetration depth, at least for the range of speed studied here.

Additionally, the wave speed also affects the shape of the perturbation velocity field. The shape of the spanwise component is intuitive since it largely follows the pattern of the background uncontrolled laminar flow in the moving frame of reference. For low wave speeds, in the moving frame of reference, the background flow is in the positive streamwise direction in most of the domain, causing the spanwise velocity structures to tilt in that direction. For $c^* = 1$, in the moving frame of reference, the background flow is in the negative streamwise direction near the walls and in the positive streamwise direction near the center of the channel, and the spanwise velocity structures reflect this. For large wave speeds, in the moving frame of reference, the background flow is in the negative streamwise direction throughout the domain, causing the spanwise velocity structures to tilt in that direction. The streamwise and wall-normal velocity structures, however, have more complicated shapes that do not conform to this intuition, and further investigation is required.

Finally, we remark on the potential for net energy savings relative to the uncontrolled laminar flow. According to Eq. (1), the control term must be greater than the rate of dissipation of the perturbation velocity field. The ratio of these two terms is tabulated for all of the simulations in Table 1, and we refer to it as the power ratio; a value greater than 1 would indicate net energy savings relative to the uncontrolled laminar flow. For the parameter values used here, the uncontrolled laminar flow is energetically superior. Note that the numerator of the power ratio is independent of the wave speed c^*, depending only on

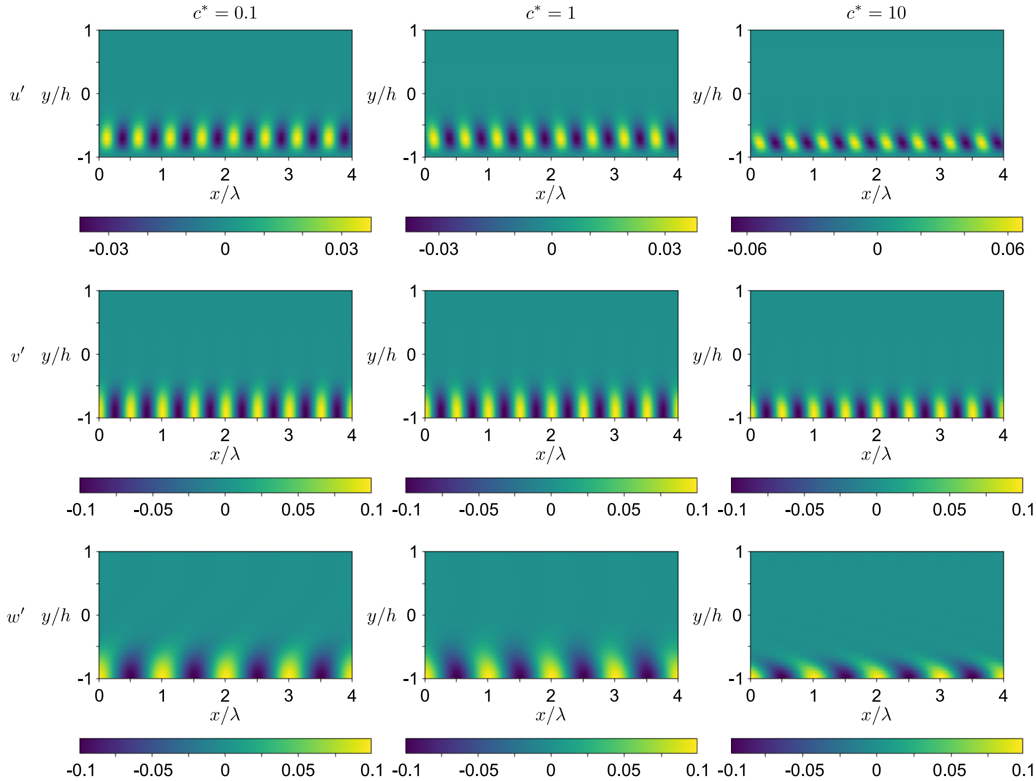

Figure 4. Perturbation velocity in the frame of reference moving with the travelling waves, for $k^* = 10$ Each row shows a different velocity component, and each column corresponds to a different wave speed.

the wavenumber k^*, while the dissipation in the denominator depends on both parameters. The ratio of the two terms is far from 1, so we hesitate to make any firm conclusions. However, we do observe that the dissipation of the perturbation velocity field increases with the wave speed of the control, and especially increases with the wavelength. One can clearly see that a larger penetration depth of the perturbation velocity field will yield greater dissipation. An important point to observe is that the power ratio scales with the Reynolds number (at least superficially; the denominator will have a non-trivial scaling with the Reynolds number that we cannot predict *a priori*). We may therefore expect that larger Reynolds number provide a better opportunity for net energy savings.

Table 1. Power ratio for all cases.

k^*	c^*	$\frac{\rho\left\langle\int_{\text{walls}} w^2(\mathbf{u}\cdot\mathbf{n})\,\mathrm{d}A\right\rangle}{\mu\langle\|\nabla\mathbf{u}'\|^2\rangle}$
0.1	0.1	3.08×10^{-3}
0.1	1	3.07×10^{-3}
0.1	10	2.71×10^{-3}
1	0.1	7.03×10^{-2}
1	1	4.66×10^{-2}
1	10	3.10×10^{-2}
10	0.1	1.97×10^{-2}
10	1	1.91×10^{-2}
10	10	1.01×10^{-2}

CONCLUSIONS

Through a control volume analysis, we have extended the results of Bewley (2009) and Fukagata *et al.* (2009) to show that channel flows that are driven by pressure, shear, or a combination of the two, and controlled either by transpiration or spanwise wall motion, are subject to a fundamental limit. Specifically, the uncontrolled laminar flow gives the lower bound on energy expenditure in such flows.

Additionally, we have shown that combining transpiration and spanwise wall motion can beat this energy limit and possibly sustain sub-laminar energy expenditure, and have derived a necessary condition for net energy savings.

We then conducted direct numerical simulations to investigate what form of control can achieve net energy savings relative to the uncontrolled laminar flow. On the basis of the necessary condition for net energy savings, we constructed an actuation at the wall consisting of streamwise-travelling waves of transpiration and spanwise wall motion, with the two actuations having the same wave speed and the spanwise wall motion having twice the wavelength of the transpiration. Long waves are better able to penetrate the flow and create a significant perturbation, but also lead to greater dissipation. At the low Reynolds number simulated in this work, net energy savings relative to the uncontrolled laminar flow have proven evasive. We anticipate that larger Reynolds numbers will be more favorable to net energy savings, which we will investigate in future work.

REFERENCES

Bewley, T. R. 2009 A fundamental limit on the balance of power in a transpiration-controlled channel flow. *Journal of Fluid Mechanics* **632**, 443–446.

Burns, K. J., Vasil, G. M., Oishi, J. S., Lecoanet, D. & Brown, B. P. 2020 Dedalus: A flexible framework for numerical simulations with spectral methods. *Physical Review Research* **2** (2), 023068.

Chandran, D., Zampiron, A., Rouhi, A., Fu, M. K., Wine, D., Holloway, B., Smits, A. J. & Marusic, I. 2023 Turbulent drag reduction by spanwise wall forcing. Part 2: High-Reynolds-number experiments. *Journal of Fluid Mechanics* **968**, A7.

Floryan, D. 2023 A fundamental limit on energy savings in controlled channel flow, and how to beat it. *Journal of Fluid Mechanics* **954**, R3.

Fukagata, K., Sugiyama, K. & Kasagi, N. 2009 On the lower bound of net driving power in controlled duct flows. *Physica D: Nonlinear Phenomena* **238** (13), 1082–1086.

Jovanović, M. R. 2021 From bypass transition to flow control and data-driven turbulence modeling: an input–output viewpoint. *Annual Review of Fluid Mechanics* **53**, 311–345.

Kim, J. 2011 Physics and control of wall turbulence for drag reduction. *Philosophical Transactions of the Royal Society A: Mathematical, Physical and Engineering Sciences* **369** (1940), 1396–1411.

Luchini, P. & Quadrio, M. 2022 Wall turbulence and turbulent drag reduction. In *50+ Years of AIMETA: A Journey Through Theoretical and Applied Mechanics in Italy*, pp. 349–364. Springer.

Marusic, I., Chandran, D., Rouhi, A., Fu, M. K., Wine, D., Holloway, B., Chung, D. & Smits, A. J. 2021 An energy-efficient pathway to turbulent drag reduction. *Nature Communications* **12** (1), 5805.

Ricco, P., Skote, M. & Leschziner, M. A. 2021 A review of turbulent skin-friction drag reduction by near-wall transverse forcing. *Progress in Aerospace Sciences* **123**, 100713.

Rouhi, A., Fu, M. K., Chandran, D., Zampiron, A., Smits, A. J. & Marusic, I. 2023 Turbulent drag reduction by spanwise wall forcing. Part 1: Large-eddy simulation. *Journal of Fluid Mechanics* **968**, A6.